

Are all behavioral reward benefits created equally? An EEG-fMRI study

Mariam Kostandyan^{a,*}, Haeme R.P. Park^{a,b,c}, Carsten Bundt^a, Carlos González-García^a, David Wisniewski^a, Ruth M. Krebs^a, C. Nico Boehler^a

^a Department of Experimental Psychology, Ghent University, Belgium

^b Neuroscience Research Australia, Randwick, Australia

^c School of Psychology, University of New South Wales, Sydney, Australia

ARTICLE INFO

Keywords:

Reward
Monetary incentive delay task
Stimulus reward association
Cognitive control
ERP
fMRI

ABSTRACT

Reward consistently boosts performance in cognitive tasks. Although many different reward manipulations exist, systematic comparisons are lacking. Reward effects on cognitive control are usually studied using monetary incentive delay (MID; cue-related reward information) or stimulus-reward association (SRA; target-related reward information) tasks. While for MID tasks, evidence clearly implicates reward-triggered global increases in proactive control, it is unclear how reward effects arise in SRA tasks, and in how far such mechanisms overlap during task preparation and target processing. Here, we address these questions with simultaneous EEG-fMRI using a Stroop task with four different block types. In addition to MID and SRA blocks, we used an SRA-task modification with reward-irrelevant cues (C-SRA) and regular reward-neutral Stroop-task blocks. Behaviorally, we observed superior performance for all reward conditions compared to Neutral, and more pronounced reward effects in the SRA and C-SRA blocks, compared to MID blocks. The fMRI data showed similar reward effects in value-related areas for events that signaled reward availability (MID cues and C-SRA targets), and comparable reward modulations in cognitive-control regions for all targets regardless of block type. This result pattern was echoed by the EEG data, showing clear markers of valuation and cognitive control, which only differed during task preparation, whereas reward-related modulations during target processing were again comparable across block types. Yet, considering only cue-related fMRI data, C-SRA cues triggered preparatory control processes beyond reward-unrelated MID cues, without simultaneous modulations in typical reward areas, implicating enhanced task preparation that is not directly driven by a concurrent neural reward-anticipation response.

1. Introduction

Cognitive control refers to a set of superordinate cognitive functions that enable the successful coordination of more basic ones, such as sensory, attentional, and motoric processes. Specifically, it is believed to orchestrate these functions in the service of successfully performing a given task, often in face of challenges such as having to overcome habitual response tendencies or having to ignore task-irrelevant information (Botvinick et al., 2001). While cognitive control has been studied successfully for a long time already, recent years have seen an increasing interest in its interplay with motivation, which has led to a growing appreciation that motivational factors are central to successful cognitive control (for recent reviews see Botvinick and Braver, 2015; Krebs and Woldorff, 2017; Westbrook and Braver, 2015; Yee and Braver, 2018).

One of the most widely used ways of combining cognitive control tasks with a motivational manipulation is the monetary incentive delay

(MID) task (Knutson et al., 2000), in which cue stimuli indicate before every trial whether reward can be obtained (e.g., Beck et al., 2010; Chiew et al., 2016; Choi et al., 2015; Wisniewski et al., 2015). In an fMRI study using an MID task in a cognitive-control context, Padmala and Pessoa (2011) found that reward prospect in a picture-word interference task reduced response conflict, which was accompanied by increased activation in the fronto-parietal brain network, along with the ventral striatum, triggered by the cue stimuli. This activity pattern likely reflects a motivational enhancement of the proactive cognitive-control strategy described in the dual mechanisms of control (DMC) framework (Braver, 2012). The DMC framework distinguishes this proactive control strategy, which is a form of sustained maintenance of goal-directed information until the behavior is executed, and a reactive control strategy, which is characterized as a transient adaptation mechanism that is mobilized only when immediately needed (Braver, 2012; Jimura et al., 2010).

Yet, variants of the MID task, which likely lead to increased proactive

* Corresponding author. Department of Experimental Psychology, Ghent University, Henri Dunantlaan 2, 9000, Ghent, Belgium.

E-mail address: mariam.kostandyan@ugent.be (M. Kostandyan).

<https://doi.org/10.1016/j.neuroimage.2020.116829>

Received 2 August 2019; Received in revised form 5 April 2020; Accepted 5 April 2020

Available online 10 April 2020

1053-8119/© 2020 Published by Elsevier Inc. This is an open access article under the CC BY-NC-ND license (<http://creativecommons.org/licenses/by-nc-nd/4.0/>).

control for reward-related trials, are obviously not the only way in which reward can be associated with a task (for a review see Krebs et al., 2016). There is growing evidence that reward can also rapidly enhance cognitive control even if there is no time for explicit proactive preparation, e.g., in tasks that associate a feature of the target stimuli (e.g., the color) to reward, resulting in stimulus reward associations (SRA; Boehler et al., 2014; Schevernels et al., 2015; Krebs et al., 2010). At least superficially, SRA tasks are more likely to affect more reactive control functions, since participants cannot anticipate whether a given trial will be rewarded or not (Boehler et al., 2014; Janssens et al., 2016). Yet, a simple dichotomy of proactive and reactive control strategies might not fully capture the different effects of motivation during MID and SRA tasks, respectively.¹

For instance, recent EEG work using an SRA paradigm suggested an interaction of proactive and reactive control mechanisms under this reward regime (Chaillou et al., 2017; Krebs et al., 2013; Schevernels et al., 2015). In particular, Schevernels et al. (2015) argued that in the SRA task (in their case, a stop-signal task with reward being communicated by one of two stop-signal colors), a form of proactive control can still be engaged by strategically screening for a reward-related feature, which then likely accelerated reactive (inhibitory) control mechanisms. In principle, it seems possible that reward in SRA tasks triggers either enhanced reactive control and/or relies on a more specific form of proactive control (strategically preparing for the processing of reward-related features) than what is likely driving reward effects in MID tasks (globally increasing preparation for the upcoming trial). Yet, one limitation in this comparison is that in SRA contexts, preparation is hard to characterize, since there is no event that would clearly trigger preparatory processes (i.e., a cue). As a consequence, the mechanics of reward effects in SRA tasks are much less clear than during MID tasks.

Importantly, a better understanding of these different reward-triggered cognitive-control processes might come from the direct comparison of MID and SRA tasks, which has not yet been undertaken. In the present study, our main aim was therefore to directly compare them within the context of a reward-modulated Stroop task, in order to directly follow up on earlier work in this domain using Stroop or Stroop-like tasks (Krebs et al., 2013; Padmala and Pessoa, 2011). In addition, given that the literature background above identified complementary findings from fMRI and EEG work, we opted for using simultaneous EEG and fMRI recordings, which reveal relevant aspects of reward processing, task preparation, and cognitive control regarding the brain areas involved, as well as giving insights into the temporal dynamics of neural activity. Hence, both modalities provide complementary mechanistic information that is not accessible via behavioral data, and the direct combination provides such information from different angles under identical experimental conditions. While the direct combination of these techniques holds many advantages, in particular concerning their direct analytical integration (Huster et al., 2012), our main goal here was to acquire the two data modalities simultaneously, in order to obtain data from the exact same participants, at the same time and circumstances (i.e., lying down in a loud scanner environment; Debener et al., 2006). While this implies significant additional effort, and some potential signal-quality loss for the EEG data, it has been shown that cognitive-control performance is significantly affected by the MR scanner environment (Hommel, Fischer, Colzato, van den Wildenberg and Cellini, 2012), meaning that acquiring these two modalities separately introduces a systematic difference that is usually ignored.

In order to be able to triangulate different aspects related to task

¹ Note that for the pure question of characterizing reward-related differences in proactive and reactive control, other tasks than the present one might be more ideal, in particular the AX-continuous performance task (AX-CPT; e.g., Locke and Braver, 2008; Braver et al., 2009; Chiew and Braver, 2013; Chaillou et al., 2017). In the present work, however, we were particularly interested in following up earlier work using more ubiquitously-used cognitive-control tasks, here the Stroop task.

preparation and execution, we designed four different conditions that were run in separate task blocks: (i) classic MID blocks with cues being predictive of reward (independent of target-stimulus identity); and (ii) SRA blocks with target-locked reward information; (iii) we added a novel block type, called cued-SRA (C-SRA) blocks where reward-unrelated cues were included to directly match the temporal MID structure (i.e., reward was associated to specific target features as in the SRA blocks regardless of the given cue). This novel block type would allow us to characterize possible preparatory effects in an SRA context and to compare them to the MID blocks; and (iv) neutral blocks (Neutral) with a typical, reward-unrelated Stroop task, which was temporally matched to the SRA structure.

Behaviorally, we predicted global reward effects for all reward-related conditions in the respective blocks (e.g., SRA, MID, and C-SRA) in the sense of faster and more accurate responses. On a more specific level, we generally expected reductions in response-conflict effects (incongruent vs. congruent trials; e.g., Chiew and Braver, 2016; Krebs et al., 2010; Padmala and Pessoa, 2011). Moreover, for the comparison between block types, in which reward was associated to the target stimuli (SRA/C-SRA) vs. not (MID), we expected stronger reward effects for the former, due to the potential for specific enhancement of reward-related target features. Such an effect would suggest targeted preparation for specific reward-related targets, which is impossible in this specific sense in the MID blocks, in which participants would have to rely on enhancing preparation more globally.

In terms of *cue-related* predictions for the fMRI data, we expected increased activity in reward-related regions such as the ventral striatum and the associated dopaminergic midbrain, but also in frontal response-conflict regions and motor-related areas, for the MID reward-related cues compared to the MID reward-unrelated cues (Krebs et al., 2012; Padmala and Pessoa, 2011). For the C-SRA cues, we expected lower levels of activity in reward-associated regions than for MID reward-related cues, since they do not explicitly predict reward. Yet, C-SRA cues could still induce more activity than MID reward-unrelated cues even in reward-related areas, since the probability of reward is on average 50%, as two out of four target colors are reward-related. Concerning activity more directly linked to task preparation (von Cramon and Brass, 2002), C-SRA cues might also trigger enhanced preparatory activity, indicating that participants either globally increase task preparation or specifically prepare for the possibility of reward-related targets. Concerning cue-related ERPs, we were mainly interested in the cue-locked P3 component and contingent negative variation (CNV). The P3 has been linked to evaluative processes, including related to reward expectation displaying larger amplitudes for reward-related events (Goldstein et al., 2006; Hughes et al., 2013), so that we hypothesized to find enhanced P3 amplitudes for reward-related MID cues compared to the reward-unrelated MID and C-SRA cues. The CNV component, in turn, is more closely linked to preparatory-effort mechanisms, and is enhanced during the anticipation of an event of interest, in a way that probably represents a consequence of the motivational effect of reward in respective tasks (van den Berg et al., 2014). Consistent with our expectations concerning the involvement of fronto-parietal control regions that likely underlie such activity (Grent-'t-Jong & Woldorff, 2007), we again expected enhanced CNV amplitudes for reward-related MID cues compared to the reward-unrelated MID and C-SRA cues. Simultaneously, depending on what exact preparatory mechanisms the CNV reflects, we expected that it might also be enhanced for C-SRA cues compared to reward-unrelated MID cues. Yet, since preparation might take a different form (specific towards certain targets rather than global), it is unclear whether the CNV would reflect such processes.

Concerning *target-related* activity, we expected enhanced activations in reward-related areas for the reward conditions in the SRA and C-SRA blocks; however, for the MID targets, we expected less activity in the same regions, due to the fact that the preceding MID cues would have already conveyed any reward-related information. On this note, a more overarching research question was in how far reward-related brain

activity patterns for SRA targets would resemble MID cues, rather than MID targets, which would imply a procedural overlap on a different time scale. In addition, we expected less control-related brain activity during target processing for the pre-cued blocks (C-SRA and MID) compared to SRA and Neutral blocks. Concerning target-related ERPs, we hypothesized enhancements of the attention-related N1 component for reward-related trials compared to reward-unrelated ones. This prediction was based on our earlier observation in a similar context that this component is enhanced for SRA stimuli, likely reflecting the specific preparation and screening for their occurrence (Schevernels et al., 2015). Yet, it might also be modulated in MID contexts, reflecting generally enhanced attention to reward-related target stimuli (Baines et al., 2011). We further expected stronger P3 modulations in response to reward-related targets compared to reward-unrelated targets. Finally, we expected reward-related modulations of the N450 component, which is related to response conflict (Larson et al., 2014), mirroring our behavioral conflict-related (i.e., congruency-related) predictions.

In sum, the present study aimed at exploring how different ways of associating reward to a cognitive-control task would impact behavior, and whether such potential differences would be brought about by identifiably dissociable mechanisms as reflected in the fMRI and EEG data. Such differential mechanisms could relate to how and when reward is represented, as well as to changes in how exactly cognitive control is exerted in the sense of globally or target-specifically increasing proactive control, reactive control, or moderating an interaction between those control modes.

2. Methods

2.1. Participants

Twenty-eight native Dutch speaking volunteers with no history of psychiatric or neurological disorders and with normal or corrected-to-normal vision took part in the experiment for honorarium. During recruitment, participants had to fill out a screening questionnaire provided by the Ghent Institute for Functional and Metabolic Imaging; exclusion criteria were cardio-vascular problems, fever, current use of medication, recent surgery, metal/electronic implants, cardiac pacemakers, and neuro-stimulators. From the 28 participants that ultimately took part in the study, three were excluded from all analyses due to excessive movement in the scanner (more than 3 mm of translation or more than 3° of rotation), resulting in a final sample of 25 participants (13 men, age $M = 23$, $SD = 2.94$, one left-handed). Prior to participation, all participants gave written informed consent. The study was approved by the ethical committee of the Ghent University Hospital.

2.2. Design and procedure

Participants performed a rewarded Stroop task based on earlier work by Krebs et al. (2010), with a systematic extension to include the four different block types mentioned in the Introduction (MID, C-SRA, SRA, and Neutral blocks; see next paragraph for details). Throughout the entire experiment, a fixation dot was displayed in the middle of the screen, and stimuli were presented directly above it. All stimuli were presented in Dutch and were randomly chosen from the following set of capitalized colored words: GEEL, ROOD, BLAUW, GROEN (yellow, red, blue, green). Word meaning was either congruent or incongruent with the ink color, and participants had to respond manually to the ink color irrespective of the word meaning. In order to simplify the counterbalancing and avoid contingency learning (Duthoo et al., 2014), we used two different sets of incongruent stimuli: (i) first set – GROEN (in red ink), ROOD (in yellow ink), BLAUW (in green ink), GEEL (in blue ink); and (ii) second set – GROEN (in blue ink), ROOD (in green ink), BLAUW (in yellow ink), GEEL (in red ink). This also allowed us to present each incongruent stimulus in a reward-related color and a reward-unrelated color. The cues consisted of three “euro” signs (€) vs. three zeros (0) in

the MID block (for the reward-related vs. reward-unrelated conditions, respectively) and three “at” signs (@) vs. three ampersands (&) in the C-SRA block (the latter was included merely in order to match the general two cue type structure in the MID condition, but here both cue types served only as a general preparation cue with no reward meaning).

The experiment consisted of four different block types: SRA blocks, Neutral blocks, C-SRA blocks, and MID blocks. In all block types, participants performed a regular Stroop task by reporting the ink color of color words. Participants responded with four buttons on an MR-compatible button box, which was placed under both hands of the participants inside the MRI scanner. Importantly, the timing was adjusted such that the rate of targets was the same in all blocks (with an average SOA of successive targets of 6.1 s). The nature of these different block types was explained to the participants, and they were told that the number of target stimuli would be identical in all blocks (resulting in a generally faster event rate for blocks involving cue stimuli, but a fixed target rate, yielding the same possibility of garnering monetary bonuses in all reward-related blocks). The buttons under the middle and index fingers of the left hand were mapped to blue and yellow, whereas the buttons under the middle and index fingers of the right hand were assigned to green and red (while the association of reward to the colors was counterbalanced across participants, this general color-response set-up was kept constant across all participants for the sake of simplicity). Participants were instructed and briefly trained on the task outside of the scanner, and were then informed about the reward manipulations in the different blocks. Participants were asked to respond as fast and as accurately as possible, and to consider the offset of the target stimulus (after 700 ms, see below) as the approximate response deadline.

In the SRA blocks (see Fig. 1A) target stimuli were presented for 700 ms, followed by an inter-trial interval varying randomly from 2700 to 10300 ms. Each ITI value consisted of one of seven possible values drawn from a pre-specified distribution ($M = 5.4$ s, $SD = 2.1$ s) plus an additional small random jitter of 0–100 ms (equally distributed) serving to further de-correlate the EEG data from the MR data acquisition. Two out of the four ink colors (red/yellow or blue/green) were potentially rewarded, i.e., participants could win a monetary bonus for fast and accurate responses. The other two ink colors (blue/green or red/yellow) were reward-unrelated. The reward-related colors were counterbalanced across participants.

The set-up and timing of events in the Neutral blocks were identical to the SRA blocks (see Fig. 1B) without any reward, hence yielding a classic Stroop task.

Trials in the C-SRA blocks (see Fig. 1C) started with a cue stimulus that was presented for 300 ms. Here, the cues did not hold any information about reward availability but represented an attentional alerting signal simply indicating the upcoming appearance of the stimulus. After the cue, a cue-target interval lasted for varying durations from 2000 to 7000 ms (drawn from a pre-specified distribution of four possible values with more short than long SOAs, $M = 3.3$ s, $SD = 1.6$ s). Then, the Stroop target word was presented for 700 ms followed by an inter-trial interval of 1650–2050 ms (equally distributed). Again, as in the SRA block, the reward information was target-locked and the reward-related/reward-unrelated colors were counterbalanced across participants.

The timing of MID blocks was identical to that of the C-SRA block (see Fig. 1D). However, unlike the C-SRA blocks, the reward information was communicated via the cues (and independently of target identity). Specifically, “euro” signs predicted reward in case of a fast and correct response while zeroes predicted no reward, no matter the performance. The ink color of the words did not matter for the potential gain of reward (however, obviously, participants still had to respond to the color of the word).

In SRA, MID, and C-SRA blocks, participants were rewarded with seven cents for each correct and fast response to a reward-related trial, which could result in a maximum bonus of €10, and were neither rewarded nor penalized for incorrect or slow responses. While participants were instructed to respond within the 700-ms stimulus

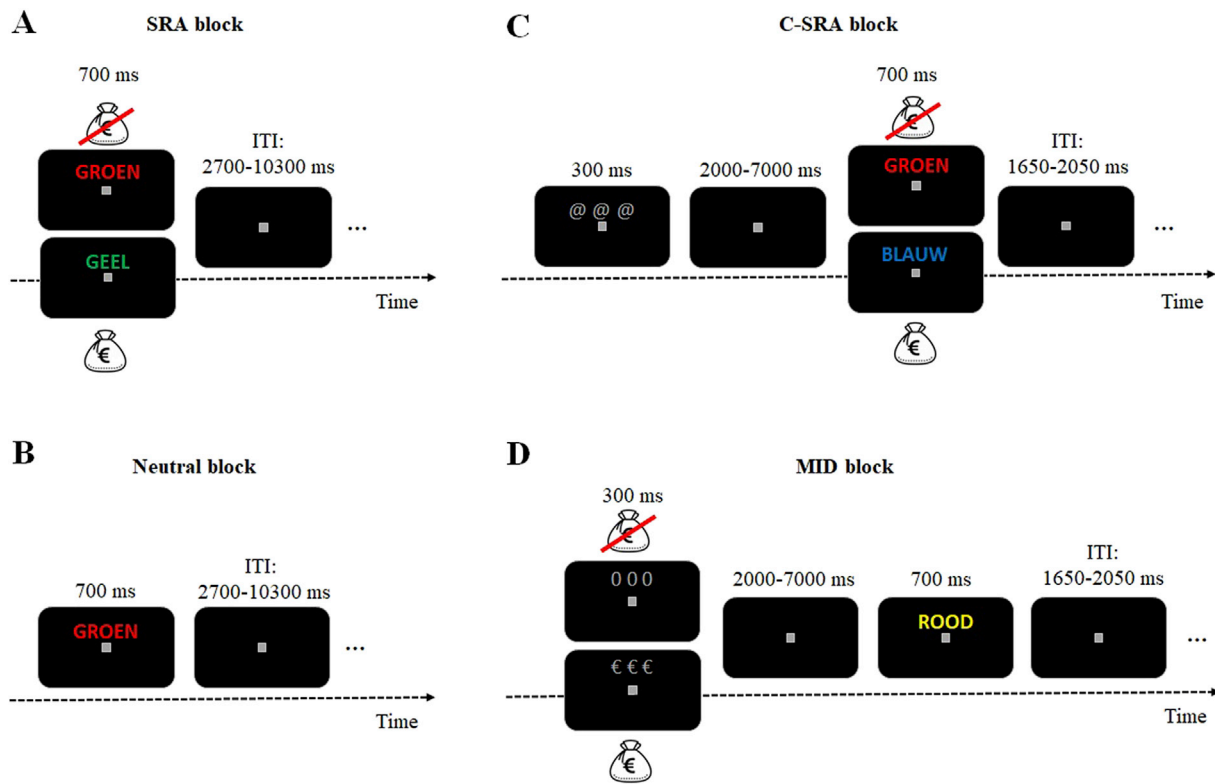


Fig. 1. Paradigm in the different block types (groen, geel, blauw, and rood are Dutch for green, yellow, blue, and red, respectively). Mean SOA for subsequent targets was kept constant at 6.1 s across all block types. (A) In the SRA blocks reward was associated with colors of the target stimuli (e.g., green and blue color = reward-related; red and yellow color = reward-unrelated). (B) Neutral blocks were identical to the SRA blocks, but without any reward association. (C) In C-SRA blocks, the color of the target stimulus again carried the reward information, while the cues only served an attentional alerting function. (D) In the MID block, cues indicated reward availability (for which target color was irrelevant), i.e., “euro” signs indicated potential reward-related trial, while zeroes signaled no reward.

presentation, which was also used to calculate participants’ reward bonus, we used a slightly wider time-window for scoring trials as correct or incorrect for the ultimate analysis of the behavioral data (accepting responses between 100 and 1000 ms post stimulus onset). This wider window was used in order not to confound accuracy with response speed, leaving only a very low number of misses (less than 2% of trials). Since the number was low, we simply scored those trials as misses and included them in the calculation of accuracy, meaning that accuracy is the proportion of correct trials within the above time window from all trials, without further subdivision. In all reward-related blocks, cumulative reward feedback in the form of the accumulated reward bonus up until this point was presented every 16 trials, as we have done in this context before (e.g., Krebs et al., 2011). At the corresponding times in Neutral blocks, feedback always showed a cumulative reward bonus of zero.

All blocks were presented in a random order throughout the experiment, and fully randomized across participants. There were six runs in total, each consisting of four blocks. Each block comprised of 16 trials and the ratio for reward-related and reward-unrelated trials was equal (50%/50%) in the MID, the SRA, and the C-SRA blocks. The same was true for the number of congruent (50%) and incongruent (50%) trials in all four block types. In order to still appropriately sample the hemodynamic response to the respectively last event in a run, each run ended with a fixation-only screen for 12 s, followed by a 4-s presentation of the word “End” and the cumulative reward feedback.

The experiment was programmed in and controlled by Presentation® (Version 18.1; Neurobehavioral Systems; www.neurobs.com) and projected onto a screen behind the MRI scanner that was visible via a mounted mirror on the head coil.

2.3. fMRI recording

MR data were acquired using a 3 T scanner (Siemens Magnetom Trio, Erlangen, Germany) using an 8-channel head coil. Subjects were positioned head-first supine inside the magnet bore. For communication and noise cancellation, we used OptoACTIVE noise-canceling MRI headphones and a FOMRI-III noise-canceling microphone (OptoACTIVE, Optoacoustics Ltd, Moshav Mazor, Israel).

For blood-oxygen level dependent (BOLD) imaging, T2*-weighted echo-planar imaging (EPI) sequence was used (TR = 2240 ms, TE = 30 ms, FA = 80°, 35 axial slices, voxel size 3.0 × 3.0 × 3.0 mm, interleaved acquisition, FOV = 192 × 192 mm, matrix = 64 × 64). A total of 206 functional volumes were acquired per run per subject. Before the functional scanning a T1-weighted MPRAGE high-resolution anatomical image was acquired (TR = 1550 ms, TE = 2.39 ms, FA = 9°, 176 sagittal layers, voxel size 0.9 × 0.9 × 0.9 mm, FOV = 220 × 220 mm, matrix = 256 × 256). Total scanning time, including a localizer, T1 structural scan, and 6 functional runs, was about 60 min.

2.4. fMRI data processing

To allow the scanner to reach steady-state magnetization, the first four images in each series were removed before analysis. The fMRI data were analyzed using SPM12 (Statistical Parametric Mapping; <http://www.fil.ion.ucl.ac.uk/spm/>). The pre-processing steps consisted of slice-time correction of the functional images; realignment of functional images; spatial coregistration of the anatomical image to the mean of the functional images; segmentation and spatial normalization of the coregistered anatomical image to the standard Montreal Neurological Institute (MNI) space (re-sampled to 1 × 1 × 1 mm voxels);

normalization of the functional images to MNI space using the deformation fields from the segmentation step; and smoothed with an 8 mm full-width at half maximum (FWHM) Gaussian kernel.

For the first-level statistical analysis, we concatenated the fMRI runs into one session using the spm12 function *spm_fmri_concatenate*, in order to account for the fact that the different block types were fully and independently randomized across different participants. This procedure adds run regressors and adjusts high-pass-filter and non-sphericity estimates. Importantly, our design furthermore prevented possible problems caused by difficult-to-capture overlap from late events in a given run by having a long blank period at the end of each run. While in theory, the present design could have qualified for a mixed block/event-related analysis that simultaneously accounts for transient and block-level effects (Petersen and Dubis, 2012; Visscher et al., 2003), it was not explicitly optimized for this, and only transient effects were analyzed. BOLD responses were modeled by delta functions at the cue and target onsets, which were then convolved with a canonical hemodynamic response function (HRF), and estimation was done including a 128-s high-pass filter. Transient effects were modeled in the GLM for the four cue conditions (C-SRA: two cue types, later combined to one; MID: reward-related vs. reward-unrelated cues) and each of the 20 target conditions (i.e., four reward \times congruency conditions in C-SRA, SRA, and MID, and congruent vs. incongruent for Neutral blocks).

The SRA and C-SRA blocks consisted of four conditions each: reward-related congruent, reward-related incongruent, reward-unrelated congruent, and reward-unrelated incongruent. As we observed reward-color transfer effects in the MID and Neutral blocks (i.e., a behavioral benefit for colors that were associated to reward in the SRA and C-SRA blocks despite this being irrelevant for MID and neutral blocks; see Supplementary section S1.2.1), we additionally split up the respective conditions in order to investigate whether the reward-color transfer was also present in the fMRI data by splitting the MID block into eight conditions: (i) reward-related congruent: reward associated color (*MID_R_rewcol_con*), (ii) reward-related congruent: no-reward associated color (*MID_R_nrcol_con*), (iii) reward-related incongruent: reward associated color (*MID_R_rewcol_inc*), (iv) reward-related incongruent: no-reward associated color (*MID_R_nrcol_inc*), (v) reward-unrelated: congruent reward associated color (*MID_U_rewcol_con*), (vi) reward-unrelated congruent: no-reward associated color (*MID_U_nrcol_con*), (vii) reward-unrelated incongruent: reward associated color (*MID_U_rewcol_inc*), (viii) reward-unrelated incongruent: no-reward associated color (*MID_U_nrcol_inc*). The neutral block included four conditions: (i) congruent: reward associated color (*Neut_rewcol_con*), (ii) congruent: no-reward associated color (*Neut_nrcol_con*), (iii) incongruent: reward associated color (*Neut_rewcol_inc*), and (iv) incongruent: no-reward associated color (*Neut_nrcol_inc*).

Only correct trials were considered for analyses (using the same time-window of 100–1000 ms post target onset used also for the analysis of the behavioral data); all incorrect trials and trials with no responses were modeled as regressors of no interest. Group analysis was performed using a one-way ANOVA with all conditions (i.e., in a fashion that did not specify an actual factorial design, which was not possible due to the fact that not all factors were fully crossed throughout the design, and because not all block types had the same events, with only half of them featuring cue stimuli) for voxel-wise comparisons [cluster-level FWE correction at $p < 0.05$; auxiliary cluster-forming p -value threshold $p < .001$, except where stated otherwise].

2.5. ROI analysis: reward and congruency effects between block types

A region of interest (ROI) analysis focusing on possible differences between conditions in reward-related and congruency-related areas was performed. Reward-related ROIs were identified from the general reward $>$ no reward (R $>$ NR) contrast, where we included targets from the MID, SRA, and C-SRA blocks and cues from the MID blocks. Congruency-related ROIs were extracted from the general incongruent $>$

congruent (inc $>$ con) contrast based on the targets of all block types including the Neutral block. Using standard thresholding [cluster-level FWE correction at $p < 0.05$; auxiliary cluster-forming p -value threshold $p < .001$], both contrasts yielded two clusters spanning across multiple anatomical areas. Due to the lack of regional specificity, we decided to apply more stringent cluster-forming thresholds for the clusters, in order to separate them into more meaningful anatomical units [still FWE cluster-level-corrected $p < 0.05$; for more details of thresholds and ROI; see Supplementary Table S1].

In addition, we defined anatomical ROIs for the dopaminergic midbrain, which included both bilateral substantia nigra (SN) and bilateral ventral tegmental area (VTA), based on a clear a-priori interest in this region related to its central role in reward-related processes and the fact that due to its small size it tends to not be identified by whole-brain voxel-wise analyses (e.g., Bunzeck and Duzel, 2006). Specifically, we used ROIs identified and hand-drawn on the SPM12 template T2 image. Note that anatomical T2 (or related) sequences are not allowed when participants wear an EEG cap in the scanner. We combined these regions in one ROI for the analysis (max/min x (mm): $-14/14$; max/min y (mm): $-20/-8$; max/min z (mm): $-14/-8$; volume: 952 mm^3), given that in humans they form a complex without a clear functional distinction (Duzel et al., 2009). Considering the relatively small size of this anatomical area, we paid special attention to the quality of our spatial co-registration and normalization procedures, in order to ensure the anatomical accuracy of our group-level ROI approach (rather than using individual ROIs).

The ROIs were created using MarsBar (<http://marsbar.sourceforge.net/>). MarsBar was also used to extract mean beta values from each ROI. In order to avoid circularity, analyses based on functionally-defined ROIs (i.e., R $>$ NR and inc $>$ con) did not consider the respective main effects of reward and congruency that were used to derive these ROIs, which for balanced designs are orthogonal to the other factors in the same ANOVA (Kriegeskorte, Simmons, Bellgowan, Baker, 2009; Poldrack, 2007). In contrast, the anatomically defined SN/VTA ROI was analyzed with regard to both experimental factors.

2.6. EEG recording

Simultaneous EEG was recorded using a 64-channel BrainCap-MR EEG cap with the MRplus amplifier (Brain Products, GmbH, Munich, Germany) at a sampling rate of 5 kHz. All 64 channels were recorded with FCz as reference and I_z as ground. Electrode impedances were kept below 10 k Ω . A SyncBox (Brain Products, GmbH, Munich, Germany) was used to further synchronize MR and EEG data acquisition. Note that our cap layout does not include a dedicated electrocardiography (ECG) channel, which is usually placed on the participants back, as well as no electrode below one of the eyes (e.g., Green et al., 2017). Those electrodes tend to be particularly noise-prone, due to the long cables and the possibility of movement. In return, our caps include two additional scalp electrodes (in our case PO9 and PO10, which are not part of the standard layout).

2.7. EEG processing

EEG data were analyzed offline using Brain Vision Analyzer (BVA) 2.1 (Brain Products GmbH, Munich, Germany). The data were corrected for MR imaging gradients (Allen et al., 2000), down-sampled to 500 Hz and re-referenced to the average of all channels.² Subsequently, we performed a raw-data inspection, excluding stretches of the continuous data that were clearly affected by large artifacts, such as residual gradient

² All channels were included into the new reference: AF3, AF4, AF7, AF8, AFz, C1, C2, C3, C4, C5, C6, CP1, CP2, CP3, CP4, CP5, CP6, CPz, Cz, F1, F2, F3, F4, F5, F6, F7, F8, FC1, FC2, FC3, FC4, FC5, FC6, Fp1, Fp2, Fpz, FT7, FT8, Fz, O1, O2, Oz, P1, P2, P3, P4, P5, P6, P7, P8, PO10, PO3, PO4, PO7, PO8, PO9, POz, Pz, T7, T8, TP10, TP7, TP8, TP9.

artifacts, which can result from a sudden movement during a given fMRI volume. Then, an independent component analysis (ICA) was performed to identify an IC that would be reflective of the cardiobalistic (CB) artifact based on the scalp EEG, rather than on an explicit ECG channel (for a similar approach see [Castelhamo et al., 2014](#)). This IC (or multiple ones) was then used to place cardio markers in a semi-automatic way, using the routines provided by BVA. Prior to the subsequent inverse ICA, we also excluded a blink IC, if present. Next, the data were exported to EEGLAB (v13.6.5b; [Delorme and Makeig, 2004](#)) and the FMRIB plug-in was used for an optimal basis set correction of the CB artifact based on the cardio markers placed prior, using four principal components ([Debener et al., 2005](#); [Niazy et al., 2005](#)). Finally, residual cardiac activity was removed based on an additional ICA, with cardio-related ICs being identified by the CB correction solution (CBC Parameters in Brain Vision Analyzer). After a final raw data inspection aimed at excluding stretches of residual artifact-related data, the data were segmented in two ways: first, into 1400 ms epochs, which included a 200 ms pre-stimulus baseline time-locked to targets, and also into 2200 ms epochs including a 200 ms pre-stimulus baseline time-locked to cues. Finally, we applied basic artifact rejection on the resulting epochs, excluding epochs with voltage changes exceeding 200 μV in a moving 100-ms time-window. Note that all processing steps were blind towards the conditions of the experiment. Corresponding to the fMRI data, only correct trials were included in the analysis.

Statistical analyses were run on baseline-corrected conditions-wise averages. The cue-locked P3 component was quantified averaged across the P1, P2, PO3, PO4, Pz, and POz electrodes, using a time-window between 300 ms and 600 ms post-cue ([Glazer et al., 2018](#); [Kostandyan et al., 2019](#); [Schevernels et al., 2014](#)). The cue-locked CNV component was examined by averaging the signal of FCz and Cz electrodes averaged over time starting at 700 ms post-cue ([Schevernels et al., 2014](#); [van den Berg et al., 2014](#)) until the moment of the minimum possible cue-target SOA jitter at 2300 ms (i.e., until the earliest possible target presentation). We chose several ERP components of interest for the target-locked component analysis based on previous research: the target-locked N1 component averaged across posterior channels PO7 and PO8 between 160 and 200 ms ([Heinze et al., 1990](#); [Tan et al., 2014](#)); the target-locked P3 component averaged across frontal Fz, FC1, FC2, F1, F2, FCz electrodes between 280 and 400 ms ([Krebs et al., 2013](#); and different to the cue-locked P3 component mentioned above); and the target-locked N450 component averaged across Cz, CP1, CP2, and CPz electrodes within a time window of 350–500 ms ([Liotti et al., 2000](#)). For presentation purposes, the data were filtered with a 20-Hz low-pass filter, whereas the statistical analyses were performed on the unfiltered data.

3. Results

3.1. Behavior

Our main analysis of interest was the comparison of the different reward-related blocks (which all featured the same general factorial design of reward and congruency), and only subsequently comparing them to the Neutral blocks (see [Supplementary section S1.1.1](#)). The average RTs and error rates were hence analyzed using a $3 \times 2 \times 2$ repeated-measures ANOVA (rANOVA) with factors block type (C-SRA vs. SRA vs. MID), reward (reward-related vs. reward-unrelated trial) and congruency (congruent and incongruent trials). Only correct responses were included in the RT analyses. For this set of analyses, we expected generally superior behavior for reward-related trials, both concerning performance in general and smaller conflict effects in the three different block types. Moreover, we expected such effects to potentially be stronger in the SRA-type blocks, given that preparation could be specifically targeted towards a subset of target stimuli.

An overview of the main descriptive statistics is presented in [Supplementary Table S1](#) and [Fig. 2](#). Globally, we observed strong main effects of reward with faster RTs in the reward-related than in the reward-

unrelated trials [$F(1,24) = 61.65, p < .001, \eta_p^2 = 0.72$] and congruency effects with faster RTs in the congruent than in the incongruent trials [$F(1,24) = 80.62, p < .001, \eta_p^2 = 0.77$; see [Fig. 2A](#)]. We also found a main effect of block type [$F(2,48) = 8.66, p = .001, \eta_p^2 = 0.27$], indicating globally faster RTs in MID [$M = 588.01, SD = 59.67$] and C-SRA [$M = 581.93, SD = 73.27$] compared to SRA [$M = 599.13, SD = 68.17$]; however, post-hoc t-tests indicated only trend-level results for each individual effect, $p > .07$. This main effect was further qualified by a significant reward \times block type interaction [$F(2,48) = 15.59, p < .001, \eta_p^2 = 0.39$], showing significantly larger reward effects in the SRA and C-SRA blocks compared to the MID block [all $p < .001$], with C-SRA and SRA showing comparable reward benefits [$p = .94$]. No other significant interactions were found [all $p > .08$]. The corresponding $3 \times 2 \times 2$ rANOVA on the accuracy data yielded a significant main effect of reward, with higher accuracy in the reward-related trials compared to the reward-unrelated trials [$F(1,24) = 13.61, p = .001, \eta_p^2 = 0.36$], a main effect of congruency with higher accuracy in congruent trials than in incongruent trials [$F(1,24) = 14.37, p = .001, \eta_p^2 = 0.37$]. Furthermore, there was a significant reward \times block type interaction [$F(2,48) = 4.40, p = .018, \eta_p^2 = 0.15$; see [Fig. 2B](#)] related to a larger reward effect in SRA than in MID [$p = .002$] and similar reward effects between MID vs. C-SRA and SRA vs. C-SRA [both $p > .1$].

We ran two additional sets of analyses, both reported in the Supplementary material (see [sections S1.1.1 and S1.1.2](#)). First, we compared the reward-related and reward-unrelated conditions from the respective blocks to the data of the Neutral trial blocks. These analyses generally found that reward-related conditions led to superior performance, also when compared to the behavior of the neutral blocks, whereas reward-unrelated conditions led to behavior very similar to that of the neutral blocks. Second, we observed color-transfer effects, both in the MID and Neutral blocks, with superior performance for trials that featured target stimuli in a color that was reward-related in the SRA and C-SRA blocks (see also [Supplementary section S1.2.1](#) for a related analysis of our fMRI data that did not identify any clear neural correlate of this effect).

3.2. fMRI results

3.2.1. ROI results: reward and congruency effects between block types

Given the complexity of our design, we decided to mostly pursue a data-driven ROI approach, identifying relevant ROIs for reward processing and for cognitive control, and then probing for possible differences across the block types. This was then supplemented by an anatomical ROI analysis for the dopaminergic midbrain. We first performed basic comparisons for the main effects of reward ($R > NR$) and congruency contrasts ($inc > con$), reported in the Supplementary material (see [section S1.2.1](#) and [Table S2](#)).

In the first ROI analysis, we extracted data from ROIs based on the global reward ($R > NR$) contrast (see [Supplementary Table S2](#)), which was based on the targets of all reward-related block types, as well as the MID cues (which already contained the reward-related information). We ran 4×2 rANOVAs on the extracted data trying to identify possible interactions between the different events in the respective block types³ (MID targets vs. C-SRA targets vs. SRA targets vs. MID cues) with reward (reward-related vs. reward-unrelated trial; note that main effects of reward were ignored given that our ROI definition was based on it). Our general hypotheses were that reward information would be represented in typical reward-related areas, and that for MID blocks, this difference would already be present during cue processing (since reward information is already fully specified then). For possible additional differences, we did not have specific hypotheses.

We observed a significant interaction reward \times block type in the bilateral CAU [$F(3,72) = 5.33, p = .006, \eta_p^2 = 0.18$] stemming from

³ For simplicity, we named this factor “block” despite the fact that we included the cues and the targets from MID block in it.

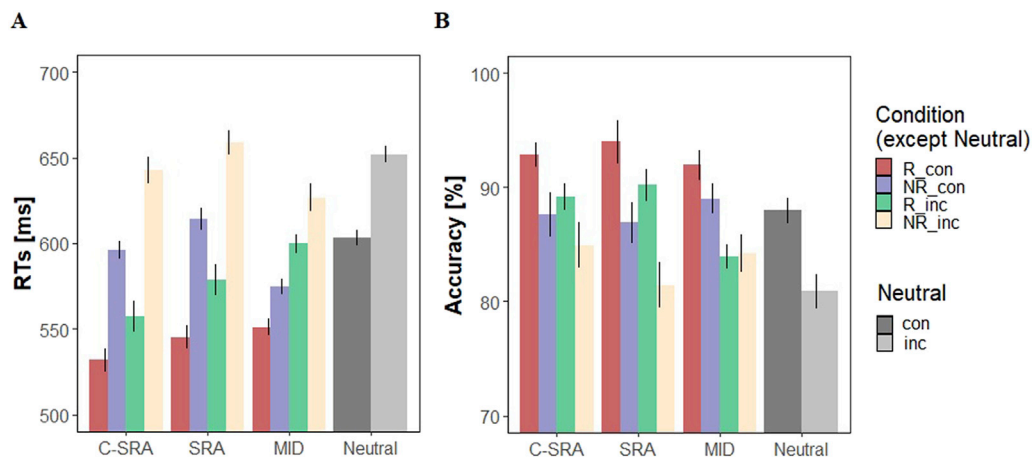


Fig. 2. Behavioral results showing mean RTs (A) and accuracy values (B) per condition and block type. Error bars represent within-subject standard error of the mean (Morey, 2008). Abbreviations of conditions: R – reward-related; NR – reward-unrelated; con – congruent; inc – incongruent.

significantly larger reward effects in the SRA targets, C-SRA targets, and MID cues compared to the MID targets [all $p < .01$; see Fig. 3A]. We also observed a significant interaction reward \times block type in the left Ins [$F(3,72) = 5.06, p = .003, \eta_p^2 = 0.17$] relating to significantly stronger reward effects in the C-SRA targets compared to the MID targets [$p = .012$] and significantly stronger reward effects in the MID cues compared to the SRA targets and MID targets [all $p < .025$; see Fig. 3B]. A similar pattern was observed in the right ORBinf [a significant interaction reward \times block type: $F(3,72) = 3.81, p = .014, \eta_p^2 = 0.14$] where higher reward effects were present in the C-SRA targets compared to the MID targets [$p = .018$] and significantly higher reward effects in the MID cues compared to the SRA targets and MID targets [all $p < .04$; see Fig. 3C]. For the bilateral dACC, the bilateral MCC, the bilateral IPG, and the right MFG we found no significant interactions [all $p > .253$].

To investigate the reward effects between block types in the dopaminergic midbrain we ran a 4×2 rANOVA with factors block type (MID targets vs. C-SRA targets vs. SRA targets vs. MID cues) and reward (reward-related vs. reward-unrelated trial; see Fig. 3). In contrast with the previous analysis, we also looked for a possible main effect of reward, as the ROI was anatomically defined (and therefore did not bias towards finding such an effect). As expected, we found a main effect of reward [$F(1,24) = 8.20, p = .009, \eta_p^2 = 0.25$] indicating significantly higher beta values for reward-related cues and targets compared to reward-unrelated trials. We also observed a significant reward \times block type interaction [$F(3,72) = 5.61, p = .009, \eta_p^2 = 0.19$] showing higher reward effects in the SRA and the C-SRA targets, as well as for MID cues, compared to the MID targets [all $p < .02$; see Fig. 3D].

Next, we investigated reward/congruency-related differences

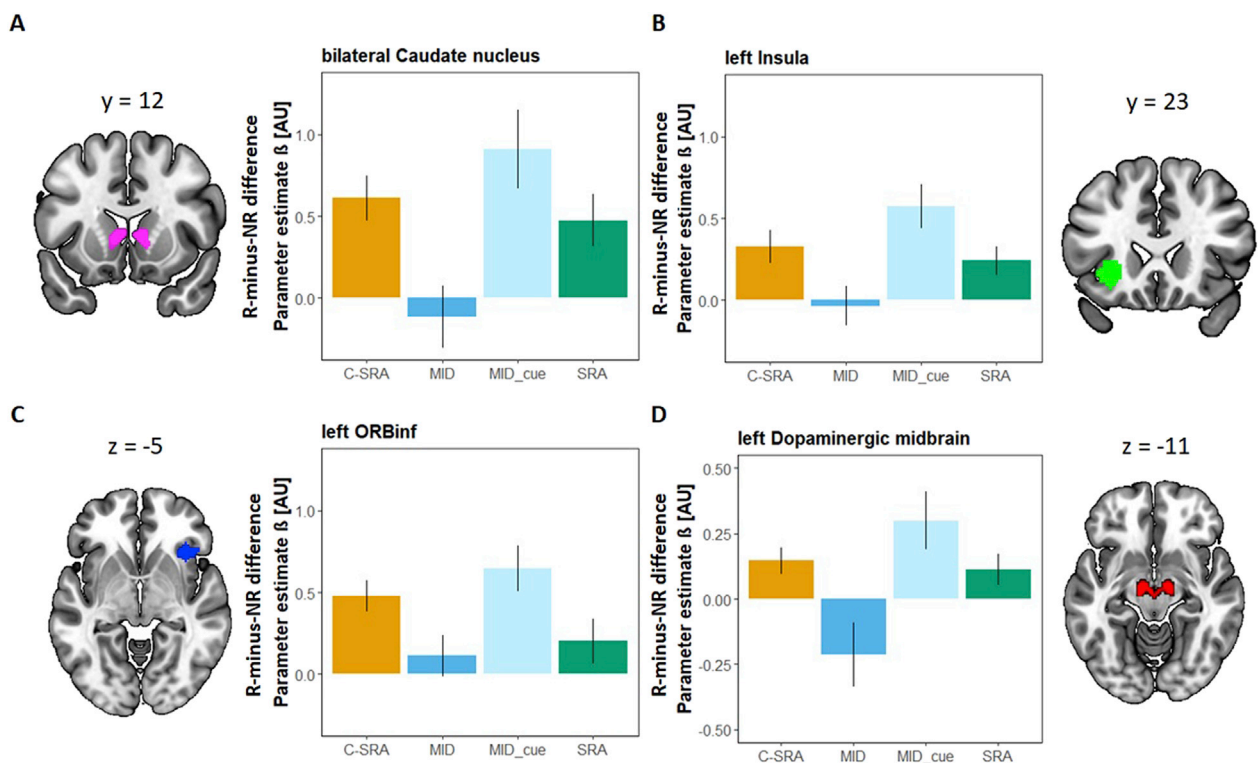


Fig. 3. ROI analyses of neural activity related to reward-related targets (C-SRA, SRA and MID blocks) and reward-related cues (MID block) in the bilateral CAU (A), the left Ins (B), the right ORBinf (C), and bilateral dopaminergic midbrain (D). Bars represent the reward-minus-no-reward differences ($R > NR$) for the C-SRA, MID, SRA targets, and MID cues. Error bars represent within-subject standard error of the mean (Morey, 2008). AU: arbitrary unit.

between blocks by extracting data from ROIs based on a global congruency (inc > con) contrast (see [Supplementary table S2](#)), which included all targets from the SRA, the C-SRA, the MID, and the Neutral blocks. Since we wanted to identify ROIs related to congruency processing and (by extension) cognitive control, we included the Neutral block in the ROI-defining contrast. At the same time, the Neutral trials were excluded from the following analysis due to our interest in the interplay between reward and congruency effects. We ran $3 \times 2 \times 2$ rANOVAs with factors block type (MID vs. C-SRA vs. SRA), reward (reward-related vs. reward-unrelated trial), and congruency (congruent vs. incongruent trials). Due to congruency being a target-related factor, these analyses exclusively investigated target-related activity. Analogous to the above analyses, we focused on possible interactions between block types and congruency, as well as on the main effects of reward and block type, and possible reward \times congruency, and reward \times block interactions. Our hypotheses were that brain areas identified based on conflict processing would also show reward effects, potentially modulated by block type. A significant reward \times congruency interaction was found in the left PreCG [$F(1,24) = 10.82, p = .003, \eta_p^2 = 0.31$] with a larger reward effect in congruent than incongruent trials ([Fig. 4A](#)). In both the right IFG and the right SPG ([Fig. 4B and C](#)), we observed higher activations for reward-related targets compared to reward-unrelated targets [main effect of reward: right IFG – $F(1,24) = 6.97, p = .014, \eta_p^2 = 0.23$; right SPG – $F(1,24) = 5.87, p = .023, \eta_p^2 = 0.20$]. In the left IPG, a significant reward \times congruency interaction was found [$F(1,24) = 5.05, p = .034, \eta_p^2 = 0.17$], stemming from a larger reward effect in congruent than in incongruent trials ([Fig. 4D](#)). No significant interactions or a main effect of reward or block type reached significant level for the bilateral PCUN [all $p > .24$].

3.2.2. Cue-level comparisons

Given the lower number of factors, and significant interest in this phase, based on the novel C-SRA condition we designed specifically to characterize task preparation also in an SRA context, we performed an additional whole-brain voxel-wise analysis time-locked to the cues to explore reward-related differences between and within MID and C-SRA

blocks (see [Table 1](#)). Hence, this analysis overlaps to some extent with the initial reward contrast (in which MID cues were also included), but exclusively focused on cue-related activity here, and additionally compared the MID cue types to C-SRA cues. We expected clear and rather widespread differences for the within-MID-block comparison in both value-related and cognitive-control brain areas. In addition, we expected that C-SRA cues would also lead to increased activity compared to MID reward-unrelated cues in some brain regions. Such differences might arise in value-related areas (since C-SRA cues imply a reward probability of 50%), but more likely in areas related to task preparation.

Within the MID block, we found increased reward-related activations in the right pallidum (Pall), the right thalamus (THA), the right superior frontal gyrus (SFG), the right thalamus (THA), the right superior frontal gyrus (SFG), the right supplementary parietal gyrus (SPG), the left PCUN, and bilateral SMA. The contrast of C-SRA cues vs. MID reward-unrelated cues revealed significant activations in the left PCUN extending to the left SPG, the left SFG, and the left IPG. Contrasting MID reward-related cues with C-SRA cues.

We found activations in the right SFG, bilateral SMA, and the left THA extending to the left Pall. Other contrasts (MID reward-unrelated cues > C-SRA cues, MID reward-unrelated cues > MID reward-related cues; C-SRA cues > MID reward-related cues) did not yield significant activations [cluster-level FWE correction at $p < 0.05$; auxiliary cluster-forming voxel-wise threshold of $p < .001$ (unc.)].

3.2.3. fMRI data summary

The present fMRI data was mainly approached with two ROI analyses. A first one, which was derived from the R > U contrast collapsed across all respective conditions (and included both MID cues and MID targets, since both could show reward effects) largely showed overlap between reward effects on MID cues and (C-)SRA targets, whereas MID targets showed much smaller (or absent) reward effects, which was also mirrored in the activity pattern of an anatomically defined ROI of the SN/VTA. A subsequent ROI analysis focusing on the interaction between reward and congruency during target processing observed main effects of

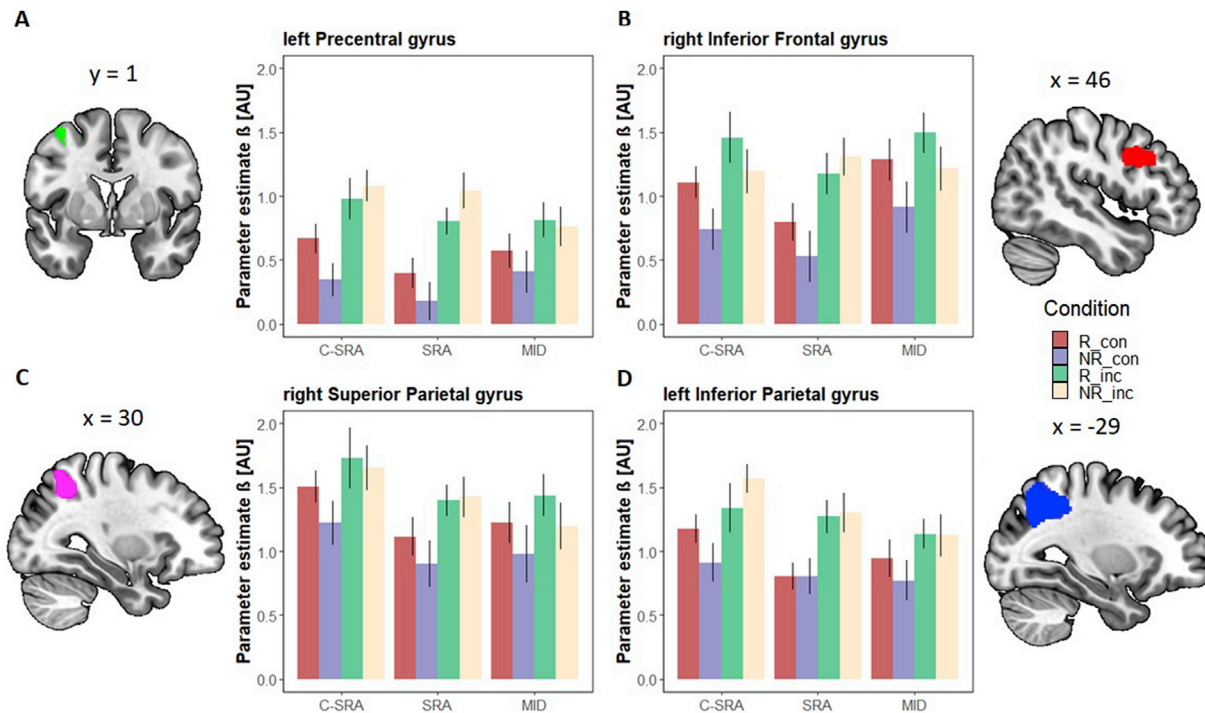


Fig. 4. ROI analyses of neural activity related to congruency in reward-related blocks in the left PreCG (A), the right IFG (B), the right SPG (C), and the left IPG (D). Bars represent the mean parameter estimate for the C-SRA, MID, and SRA targets. Error bars represent within-subject standard error of the mean (Morey, 2008). AU: arbitrary unit.

Table 1

MID and C-SRA cues within and between block types. Cluster-level FWE correction $p < 0.05$; auxiliary cluster-forming voxel-wise threshold of $p < .001$ (unc.).

	Hemisphere	k	MNI coordinates			t-value
			x	y	z	
Region						
C-SRA > MID_NR contrast						
precuneus	L	203	-3	-70	47	4.68
superior parietal gyrus	L		-18	-58	56	3.39
superior frontal gyrus, orbital part	L	88	-24	14	-13	4.60
inferior parietal gyrus	L	85	-45	-49	56	4.27
postcentral gyrus	L		-45	-34	53	3.66
Region						
MID_R > C-SRA contrast						
superior frontal gyrus	R	136	21	-1	62	5.20
precentral gyrus	R		30	-4	50	4.20
supplementary motor area	L	382	-9	-4	62	4.76
supplementary motor area	R		3	11	47	4.72
paracentral lobule	L		-12	-13	68	4.59
thalamus	L	75	-18	-13	14	4.60
pallidum	L		-21	-7	2	4.02
Region						
MID_R > MID_NR contrast						
pallidum	R	478	12	5	-1	7.80
thalamus	R		6	-19	5	6.12
supplementary motor area	R	571	3	8	50	7.57
precentral gyrus	L		-30	-7	62	6.22
supplementary motor area	L		-12	-10	65	5.45
superior frontal gyrus	R	208	24	-1	65	7.39
superior parietal gyrus	R	131	15	-64	56	6.55
precuneus	L	174	-12	-67	53	6.20
superior parietal gyrus	R		27	-58	56	5.82
inferior parietal gyrus	L		-33	-49	56	5.00
postcentral gyrus	L	78	-42	-34	53	5.45
insula	R	32	33	29	-1	5.32

Note. L: left; R: right; k: cluster size. R: reward-related; NR: reward-unrelated; inc: incongruent; con: congruent. Coordinates are in MNI space and were anatomically labelled using the MRICron (Rorden and Brett, 2000). Abbreviations of conditions: C-SRA – C-SRA cues; MID_NR – MID reward-unrelated cues; MID_R – reward-related cues.

reward in the right IFG and right SPG, and reward-by-congruency interactions in the left PreCG and left IPG, with larger reward effects for congruent than incongruent trials. Importantly, however, no interactions with block type were observed, implying similar target processing across the different block types. Finally, a voxel-wise analysis directly comparing the three different cue types observed enhanced activity in a number of areas for MID reward-related cues over both the respective reward-unrelated cues, but also over C-SRA cues. C-SRA cues, in turn, showed also some increased activity compared to reward-unrelated MID cues in a left-lateralized set of frontal and particularly parietal areas.

3.3. EEG results

3.3.1. Cue-locked components

We were first interested in reward-related differences during cue processing between the MID and the C-SRA blocks. For this, we derived ERPs of interest from previous studies and first analyzed the cue-related P3 component averaged across P1, P2, PO3, PO4, Pz, and POz electrodes between 300 ms and 600 ms. Based on its established role as a marker of valuation, we expected an exclusive increase for MID reward-related cues, although in theory, C-SRA cues might take a middle position here (given their 50% reward predictability). A one-way rANOVA with the factor cue type (MID reward-related cues vs. MID reward-unrelated cues vs. C-SRA cues) conducted on the mean amplitudes of the P3 waveform showed a main effect of cue type [$F(2,48) = 10.84, p < .001, \eta_p^2 = 0.31$]. Post-hoc pairwise *t*-test comparisons revealed an enhanced P3 for MID

reward-related cues [$M = 2.63 \mu\text{V}, SD = 1.82 \mu\text{V}$] compared both to reward-unrelated MID [$M = 1.94 \mu\text{V}, SD = 1.64 \mu\text{V}$] and C-SRA [$M = 1.89 \mu\text{V}, SD = 1.66 \mu\text{V}$] cues [post-hoc pairwise *t*-tests: both $p < .001$], which, in turn, did not differ significantly from each other (see Fig. 5A).

The analogous analysis of the cue-related CNV component averaged across FCz and Cz electrodes for the time-range between 700 and 2300 ms. We hypothesized to find enhanced CNVs for MID reward-related cues, over both other cue types, since enhanced global preparation is clearly instrumental for successful task performance. At the same time, we expected that C-SRA cues might also lead to somewhat enhanced CNV amplitudes over MID reward-unrelated cues. The analysis resulted in a main effect of cue type [$F(2,48) = 4.10, p = .023, \eta_p^2 = 0.15$], with larger CNV amplitude elicited by the MID reward-related cues [$M = -.87 \mu\text{V}, SD = 1.01 \mu\text{V}$] compared to C-SRA cues [$M = -.18 \mu\text{V}, SD = 1.27 \mu\text{V}$] and MID reward-unrelated cues [$M = -.31 \mu\text{V}, SD = 1.40 \mu\text{V}$], which, however, again did not differ significantly from each other (see Fig. 5B).

3.3.2. Target-locked components

ERP data during the target interval were analyzed to investigate the EEG correlates of reward and congruency modulations, and possible differences between MID, C-SRA, SRA, and Neutral blocks. Grand-average ERP topographic maps collapsed across the C-SRA block (reward-related and reward-unrelated targets collapsed across congruency), the SRA block (reward-related and reward-unrelated targets collapsed across congruency), and the MID block (reward-related and reward-unrelated targets collapsed across congruency and reward-unrelated cues) are illustrated in Fig. 6A and C. We first inspected the possible reward-related modulations of the N1 and P3 components, followed by the analysis of congruency-related N450 component. We generally expected enhanced N1 and P3 amplitudes for reward-related trials, which might furthermore differ across block types. For the N450, we expected amplitude modulations for reward-related trials, again with the possibility of differing across block types.

First, we probed for reward-related modulation of the attentional N1 component (averaged across PO7 and PO8 electrodes within 160–200 ms time-range was investigated by running a 2×3 rANOVA with the factors reward (reward-related vs. reward-unrelated) and block type (SRA vs. C-SRA vs. MID). We found neither clear main effects nor a significant interaction [all $p > .21$; see Fig. 6B]. Reward-related modulations of the fronto-central P3 component (averaged across Fz, FC1, FC2, F1, F2, FCz electrodes within 300–400 ms time-range; Kostandyan et al., 2019) were investigated by running a 2×3 rANOVA with the factors reward (reward-related vs. reward-unrelated trials) and block type (SRA vs. C-SRA vs. MID). We found a main effect of reward [$F(1,24) = 34.61, p < .001, \eta_p^2 = 0.59$] with enhanced P3 component for reward-related trials [$M = -.42 \mu\text{V}, SD = 2.1 \mu\text{V}$] compared to reward-unrelated trials [$M = -1.01 \mu\text{V}, SD = 2.21 \mu\text{V}$; see Fig. 6D]. We found neither a clear main effect of block nor a significant interaction [both $p > .06$].

Grand-average ERP waves of congruent and incongruent trials in the C-SRA, SRA, Neutral, and MID blocks (targets of all blocks) are illustrated in Fig. 6E. A 2×4 rANOVA with the factors congruency (congruent vs. incongruent) and block type (SRA vs. C-SRA vs. MID vs. Neutral) on the mean amplitudes of the N450 component (averaged across Cz, CP1, CP2, and CPz electrodes within a 350–500 ms time window) revealed a main effect of congruency [$F(1,24) = 10.09, p = .004, \eta_p^2 = 0.30$] with relatively more negative (i.e., here less positive in absolute terms) in incongruent trials [$M = 1.76 \mu\text{V}, SD = 2.5 \mu\text{V}$] than in congruent trials [$M = 2.1 \mu\text{V}, SD = 2.26 \mu\text{V}$; see Fig. 6F]. Neither a main effect of block nor an interaction block type \times congruency reached significance [$p > .21$].

3.3.3. EEG data summary

To summarize, the EEG data during cue processing indicated larger P3 and CNV amplitudes for MID reward-related cues compared to both the reward-unrelated MID cues and compared to C-SRA cues, which in turn did not differ. Similarly, during target processing, there was a clear main effect of reward for the fronto-central P3 component, as well as a

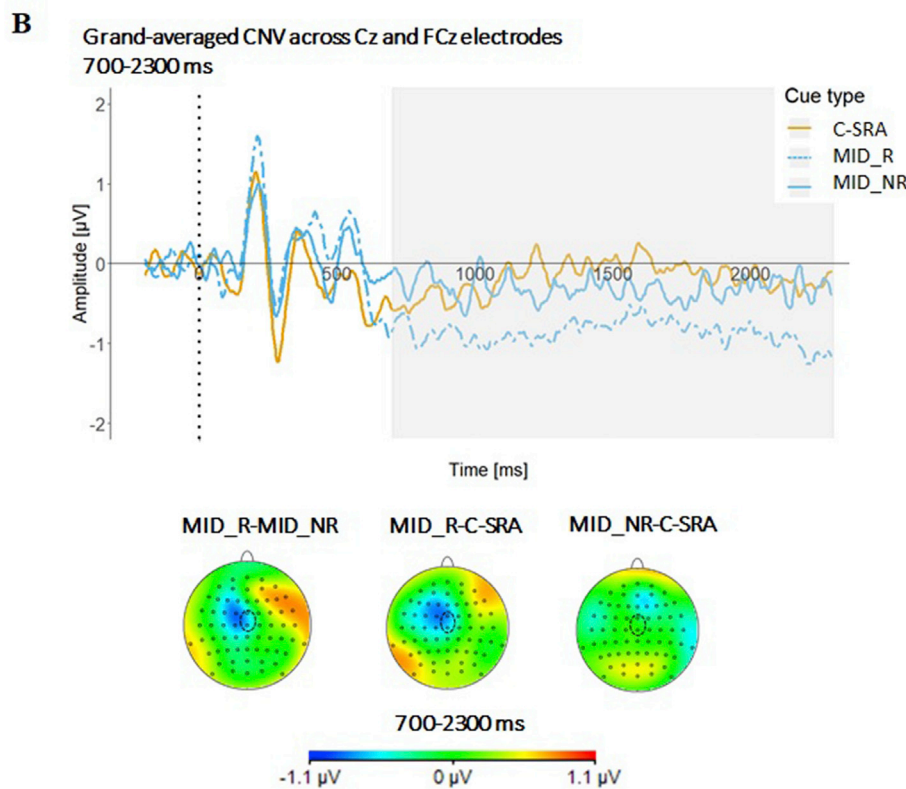
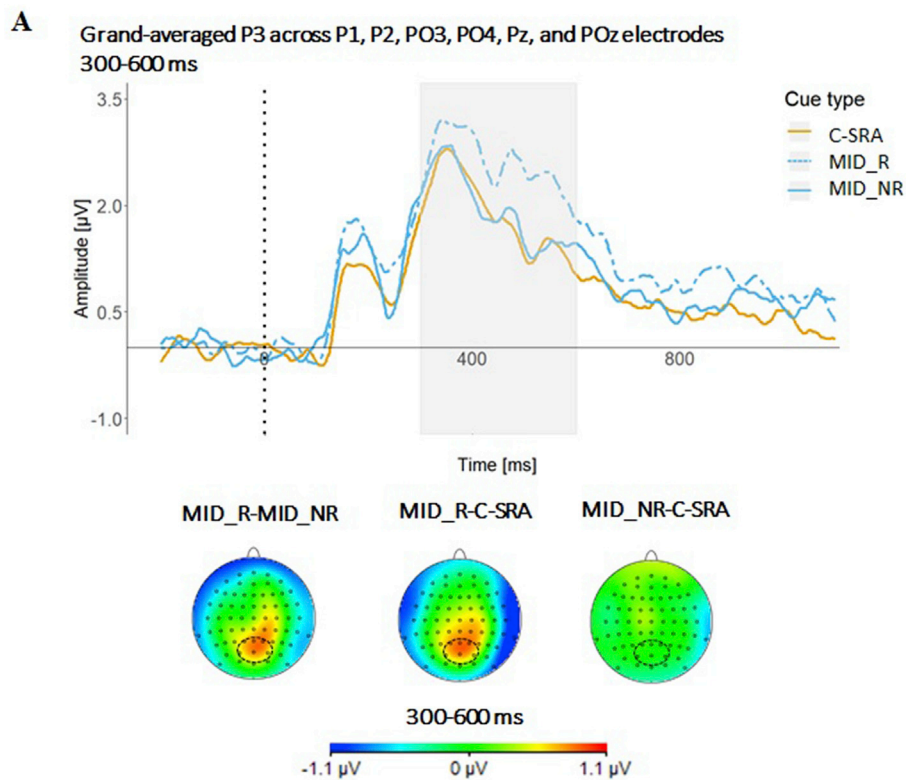


Fig. 5. Grand-averaged P3 (A) and CNV (B) waves locked all types of cues. The relevant time-ranges is highlighted by grey color. Topographies represent amplitude differences between MIDreward-related cue - minus - MID reward-unrelated cues, MID reward-related cues - minus - C-SRA cues, and MID non-rewarded cues - minus - C-SRA cues for P3 (A) and for CNV (B) components. The dashed circles on the topographic maps represent the electrodes of interest, which amplitudes were averaged for the statistical analysis. Abbreviations: R - reward-related; NR - reward-unrelated.

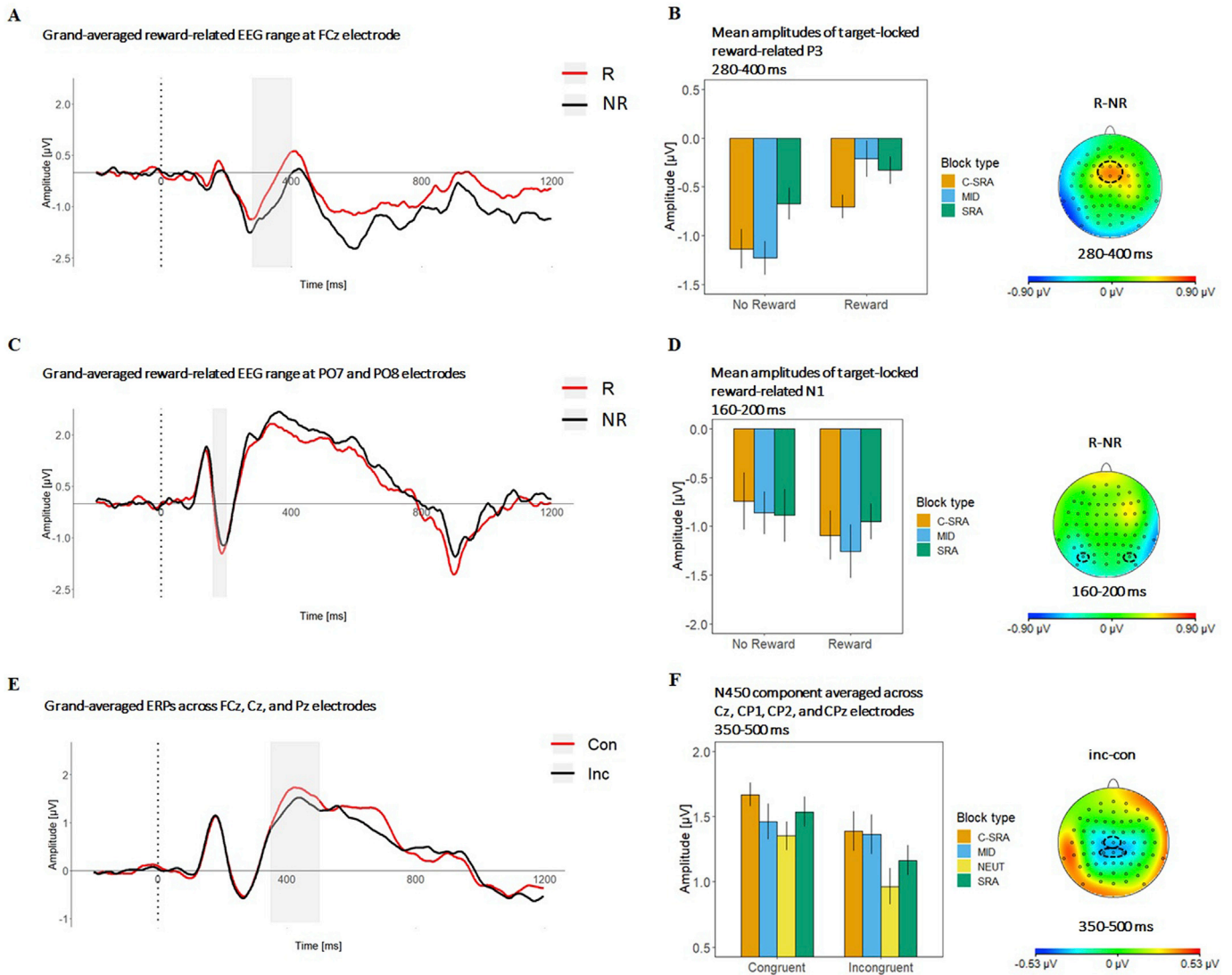


Fig. 6. Grand-averaged ERP waves time-locked to the targets (MID, SRA, and C-SRA blocks) over FCz electrode site (A) and averaged PO7 and PO8 electrodes (C) for reward-related (in red – R) and reward-unrelated trials (in black – NR). The relevant N1 and P3 time-ranges are highlighted in grey. Reward-related modulation of the P3 component in 280–400 ms time window (B) and the N1 component in 160–200 ms time window (D). The topographical maps on (B) and (D) represent the difference wave R – minus – NR. The dashed circles on the topographic maps represent the electrodes of interest, which amplitudes were averaged for the statistical analysis. (E) Grand-averaged ERP waves locked to targets (MID, SRA, Neutral, and C-SRA blocks) over averaged Fcz, Cz and Pz electrodes for congruent (con) and incongruent (inc) trials. The relevant N450 time-range is highlighted in grey. (F) Congruency-related modulation of N450 component in 350–500 ms time window. Error bars on all barplots represent within-subject standard error of the mean (Morey, 2008).

clear main effect of congruency for the N450 component. Yet, no interactions with block type were observed, along with no modulation of the attentional N1 component, which we had hypothesized to find.

4. Discussion

In the present study, we investigated the interplay between extrinsic motivation and cognitive control using a modified reward-related Stroop task with four different task blocks: MID blocks where reward prospect was communicated via advance cues; SRA blocks where the color of target stimuli signaled reward; C-SRA blocks where reward was also target-locked, but preceded by a non-informative cue (i.e., the cue did not carry reward information); and Neutral blocks that served as baseline (i.e., a regular Stroop task devoid of any reward). To investigate both spatial aspects and temporal dynamics of possible differences between these different block types concerning reward effects on cognitive control mechanisms under identical conditions, we simultaneously collected EEG and fMRI data.

Our behavioral results confirm a general reward benefit and showed typical congruency effects across all blocks. In addition, we found more pronounced reward effects in both SRA and C-SRA blocks as compared to the MID blocks, and comparable behavior in the Neutral blocks and reward-unrelated trials in all reward-related blocks. On the level of the fMRI data, we generally found that reward effects were comparable but largely observed at time periods where such information was first available (i.e., during cue processing in the MID block and during target processing in the SRA and C-SRA blocks). Concerning cue-related activity, MID reward-related cues yielded stronger activity in a set of reward- and control-related brain areas compared to both MID reward-unrelated and to C-SRA cues. C-SRA cues, in turn, also elicited stronger activity in some control-related frontal and parietal areas than MID reward-unrelated cues, but no respective difference was observed in typical value-related brain regions. These findings therefore suggest that these cognitive-control enhancements were not directly driven by a concurrent neural reward-anticipation response. Yet, beyond these differences, reward effects and their consequences on cognitive-control areas were

relatively comparable across the different block types. Our EEG data revealed a similar result pattern of expected reward effects on evaluative processes with larger amplitudes for reward-related trials (cue/target-locked P3 components), albeit in a fashion where MID targets displayed similar reward effects as C-SRA and SRA targets. Concerning preparation-related EEG activity (cue-locked CNV), we only observed increases for reward-related MID cues, whereas, counter to the respective fMRI data, C-SRA cues and MID reward-unrelated cues did not differ. During target processing, beyond the reward-related P3, we did not observe clear reward effects, and no differences across the blocks concerning attention to the target stimuli (indexed by the N1 component) or conflict processing (indexed by the N450 component). This study is the first to tackle the question of how different ways of associating reward to a cognitive-control task affects the underlying processes, and seems to largely imply that the reward effects in the different block types are in principle brought about similarly on a neural level, in particular concerning actual target processing. While this suggests some process-level unity, even if partly on different time-scales, and with some nuance concerning task preparation in (C-)SRA contexts (see below), it is important to note that not observing more pronounced reward-block interactions in the fMRI and EEG data could also relate to our analysis logic, as well as to limitations in statistical power.

4.1. Are all reward effects created equally?

Behaviorally, participants were faster and more accurate in reward-related compared to reward-unrelated trials across all reward-related blocks (MID, SRA, and C-SRA). Moreover, these reward effects represented genuine benefits compared to performance from Neutral blocks, which in turn yielded similar behavior as the reward-unrelated conditions from the reward-related block types. Our results are generally in accordance with an ever-increasing number of studies showing a beneficial effect of reward prospect on task performance in various task contexts (e.g., Adcock, Thangavel, Whitfield-gabrieli, Knutson and Gabrieli, 2006; Boehler et al., 2014; Chiew and Braver, 2013; Kim, Shimojo, & O'Doherty, 2006; Krebs et al., 2013, 2010; Ossewaarde et al., 2011).

Importantly, while there were some differences, neural reward effects as a whole were quite similar across all block types, in particular concerning target processing. This is important insofar as SRA tasks could also entail reward effects on low-level processes due to the specific association of reward with stimulus features, for which there was in fact also some evidence in the present behavioral data (the reward-related color-transfer effect described in the Supplementary material, in which reward-related target stimuli from the (C-)SRA blocks led to superior behavioral performance also in the MID and Neutral blocks, where they did not have any special status). This is in line with earlier work that has described learning of reward associations with stimuli or attentional selection processes, which appear to lead to bottom-up prioritization (e.g., Anderson et al., 2011; Chelazzi et al., 2013; Della Libera and Chelazzi, 2006). Such bottom-up prioritization can go so far as to overrule strategic considerations in attracting attention even when this is explicitly counterproductive to task performance (Hickey et al., 2010), or might trigger differential processes depending on whether or not they are relevant to the task at hand (Grueschow et al., 2015). Given the stimulus-reward association in SRA tasks (and as a consequence also to a certain response; Wang et al., 2018), it would have been conceivable that in SRA tasks reward-related trials entail *less* control-related activity than reward-unrelated trials. Yet, the present data did not indicate such a difference, rather suggesting a similar way in which reward benefits are brought about during target processing in all block types. At the same time, both C-SRA and SRA blocks featured larger behavioral reward effects than MID blocks, which probably indicates that despite the general similarity in neural implementation, there is an additional element of behavioral facilitation, which was not captured well in the current fMRI and EEG data.

Concerning cue processing and task preparation (see also next section), the question of similarity was a bit more nuanced. On the one hand,

the voxel-wise comparison of the fMRI data clearly indicated that MID reward-related cues recruited a wider network of brain areas than C-SRA cues, in particular concerning reward-sensitive areas. Still, also C-SRA cues seemed to trigger significant task preparation beyond what was observed for MID reward-unrelated cues. This speaks against a simple proactive vs. reactive dichotomy for MID and (C-)SRA tasks. As noted in the introduction, for MID-like tasks, increases in proactive control have been clearly observed (e.g., Jimura et al., 2010), as well as there being some good evidence that reward effects can be brought about very fast in a purely reactive fashion (Janssens et al., 2016). It would have therefore been possible that (C-)SRA tasks do not feature any enhanced proactive control over MID reward-unrelated cues. Still, the fact that the preparation in those trials likely was more driven by strategic orientation towards possible reward-related targets would count as evidence that there are different ways of arriving at similar (albeit not identical) behavioral reward effects, as far as such task-preparation processes go, whereas ultimate target processing seems to be similar.

4.2. The role of task preparation

In our task design, we explicitly included a block type that consisted of an SRA task, but also included a non-informative cue, i.e., the C-SRA block type. This block type was designed to match the general temporal structure of the MID task, and to account for possible alerting aspects of such cues, as well as potentially identifying preparation-related processes in a general SRA context, which is otherwise hard to capture. Specifically, although participants could not use these cues to specifically prepare for a reward-related trial, they could prepare for the possibility of such a trial, by differentially preparing for targets in the reward-related colors. Hence, by comparing the three different cues (MID reward-related, MID reward-unrelated, and C-SRA), we wanted to explore in how far preparatory processes differ along the lines of reward anticipation, expressed by generally increased preparatory control, as well as possible target-specific preparatory processes in the C-SRA case.

When contrasting the C-SRA cues with MID reward-unrelated cues, we observed activations in the bilateral PCUN and left IPG that are main functional cores of the default mode network (DMN; Mars et al., 2012; Utevsky et al., 2014; Zhang and Li, 2014), and also activations of the left superior parietal gyrus and the left orbitofrontal cortex. In contrast, comparing MID reward-related cues vs. MID reward-unrelated and vs. C-SRA cues revealed activations in areas that have been more closely linked to reward processing, including orbitofrontal PFC, superior part of the PFC, thalamus, and pallidum (Cheng et al., 2016; Cho et al., 2013; Noonan et al., 2012; Tachibana and Hikosaka, 2012). The present fMRI data are therefore consistent with the notion that task preparation differs across all of the three different cue types, and likely in a way in which only MID reward-related cues trigger a typical reward-anticipation response. Compared to MID reward-unrelated cues, both MID reward-related cues and C-SRA cues are associated with active task preparation though in a slightly different manner. Unlike MID reward-related cues that boosted reward-oriented control mechanisms associated with activations in motivation-related networks, the C-SRA cues seemed to be less reflecting reward processing and more preparation for the task, potentially oriented specifically towards the subset of targets that were reward-associated. While this makes intuitive sense, given that no reward information is provided by C-SRA cues, it is important to note that the reward expectation for the subsequent trial is 50%. As such, a graded reward-anticipation response reflecting the respective probabilities (MID_{rew} = 100%, C-SRA = 50%, MID_{nr} = 0%) would have also been conceivable. Yet, what is registered about MID cues might rather be the dichotomous fact of reward availability vs. none, whereas C-SRA cues always imply the same reward probability, which likely undermined the salience of the respective information.

In contrast to these cue-related differences in the fMRI data, we observed a less nuanced result pattern for the two cue-related EEG components we investigated. Specifically, we were interested in cue

evaluation and the subsequent preparatory processes, as reflected by the P3 and CNV component respectively (for a review see [Glazer et al., 2018](#); [Tecce, 1972](#)). Both cue-P3 and cue-CNV components were enhanced in response to MID reward-related cues as compared to MID reward-unrelated cues and C-SRA cues. C-SRA and reward-unrelated MID cues, on the other hand, did not differ for these components. The P3 modulation by the MID reward-related cue likely parallels our neuroimaging finding showing uniquely reward-related activations in motor cortex, superior fronto-parietal brain network, and thalamus, many of which are known to covary with the P3 component ([Linden, 2005](#); [Soltani and Knight, 2000](#)). In turn, an enhanced CNV component amplitude during reward-related preparation has been linked to activation within the thalamus, supplementary motor area, and prefrontal cortex ([Nagai et al., 2004](#); [Plichta et al., 2013](#)), which was also observed in our fMRI results, when contrasting MID reward-related cues against MID reward-unrelated cues and C-SRA cues. Yet, importantly, it seems conceivable that the more global preparatory processes that were increased in MID reward-related trials (i.e., preparing more strongly for any target stimulus) are better reflected in the CNV than the potentially more target-specific preparation that is likely triggered by C-SRA cues (i.e., preparing specifically for the reward-related subset of the targets). Moreover, our analysis approach for the cue-related EEG data focusing specifically on two well-characterized components might have overlooked additional differences between C-SRA and MID reward-unrelated cue processing. The idea that (C-)SRA blocks did not entail global increases in proactive control akin to that in MID blocks is furthermore supported by the absence of a reward-context effect observed in earlier work (e.g., [Jimura et al., 2010](#)). Specifically, one would have expected for (C-)SRA performance to also be superior even for reward-unrelated trials to that of the Neutral blocks, if (C-)SRA had entailed an increase in global proactive control, which was not observed here.

4.3. Reward effects on cue and target processing

When looking at target processing, we could use the data from all task blocks, although due to the factorial logic, we mostly focused on the reward effects across the three different experimental blocks (MID, C-SRA, and SRA). Starting with the EEG data, our earliest component of interest was the attention-related N1 component that can reflect processes that bridge the preceding preparation stage with the early stages of actual target processing, because it is more pronounced if participants have deployed preparatory attention ([Luck et al., 1990](#)). Specifically, based on the study by [Schevernels et al. \(2015\)](#) who observed a larger N1 for an SRA-like reward-related stimulus (in a stop-signal task), we expected more negative amplitudes for the N1 component for reward-related trials compared to the reward-unrelated ones. In addition, we expected that such a reward modulation might differ across the different reward-related blocks, in that participants could globally prepare for reward-related targets in the MID blocks, and because they could potentially prepare specifically for the possible occurrence of reward-related SRA targets. Yet, we did not observe any reward-related enhancements of the N1 component and furthermore, there was no interaction with the block type. On the one hand, it could be that a real effect was not visible due to the somewhat lower signal quality in the MR environment. On the other hand, it is quite possible that the prioritization of potential reward-related targets did not take place on this simple attentional level, not least because the task was significantly more complex than the reward-related Stop-signal task mentioned above, where a single feature (one color of a rare and highly-relevant stimulus) was reward-relevant. For the P3 component, we saw increased amplitudes for reward-related trials in all block types, albeit without differentiating among them. Based on the current data, it seems that the engagement in the task was increased whenever potentially reward-related trials were encountered ([Kostandyan et al., 2019](#); [Krebs et al., 2013](#)), irrespective of the specific reward manipulation. Additionally, we also observed expected N450 enhancement modulated by

congruency with more negative amplitudes for incongruent compared to congruent trials (e.g., [van den Berg et al., 2014](#)), which, however, again did not interact with the other factors of our design.

Looking at reward-related areas in the fMRI data (the selection of which was based on the targets from all reward-related blocks, but also the cues from the MID blocks), we observed reward-related activations in the medial prefrontal cortex (mPFC), parts of ventrolateral and dorsal prefrontal cortices (vlPFC and dlPFC accordingly), and the insular part of the orbitofrontal cortex. Moreover, we observed significant activations in the bilateral IPG, which extended to the left angular cortex. These findings are in accordance with numerous studies showing the involvement of fronto-parietal networks in reward processing and its motivation-related consequences on task processing (e.g., [Krebs and Woldorff, 2017](#)). Interestingly, in a number of areas, the reward effects were more pronounced for MID cues than for (C-)SRA targets, suggesting that reward information penetrates more deeply during the cue time-frame, probably since there is no additional task requirement at that moment (i.e., performing a discrimination task). In line with previous research, we found that reward triggered activity modulations in fronto-parietal brain regions and the dorsal anterior cingulate cortex, which are cortical structures functionally involved in the implementation of attentional control ([Cole and Schneider, 2007](#); [Corbetta and Shulman, 2002](#); [Duncan, 2010](#); [Niendam et al., 2012](#); [Power and Petersen, 2013](#)). At the same time, regions of a more purely reward-related network, such as ventromedial PFC and orbitofrontal cortex, were also activated during the reward prospect presentation (for a review, see [Ott and Nieder, 2019](#)).

The present data showed larger reward effects in the bilateral CAU and the bilateral dopaminergic midbrain for the SRA targets, C-SRA targets, and MID cues compared to the MID targets, reflecting limited reward processing for MID targets compared to SRA, C-SRA targets and MID cues. While it is typical that reward is signaled most strongly at the moment where this information is presented with no explicit reward-related activity during target processing ([Burton et al., 2015](#); [Roesch et al., 2009](#)), it seems noteworthy that the present EEG data still showed a clear reward P3 effect also for MID targets. This could indicate that the fronto-central P3 is more closely related to the implementation of a reward-related behavioral benefit (which ultimately needs to be implemented at this stage), or that there is some reactivation of the incentive information, which might be too transient or weak to be visible in the fMRI data. The overall similarity in reward-related areas across MID cues and (C-)SRA targets, however, generally implies that despite different modes of reward introduction in the task, reward information processing seems to be universal and relatively independent from reward-task associations.

When contrasting incongruent against congruent targets across all blocks, we identified a fronto-parietal network extending to the dorsal premotor cortex known to implement cognitive control mechanisms (e.g., [Banich et al., 2000](#); [Botvinick and Braver, 2015](#); [Cole and Schneider, 2007](#); [Duncan, 2010](#); [Liu et al., 2015](#); [Power and Petersen, 2013](#)). Moreover, in the left PreCG and the left IPG we observed a generally stronger reward effect in congruent trials compared to incongruent trials across all reward-related blocks. This result does not immediately fit with earlier studies that found a significant reward and congruency interaction in the mPFC ([Padmala and Pessoa, 2011](#)) and a reward influence on the Stroop effect in occipital regions and the cuneus ([Ma et al., 2016](#)). While this might be related to difference in the exact task and reward manipulation (see also next paragraph), the most relevant piece of information here is that this effect did not differ across the different block types investigated in the present study.

C-SRA and MID blocks both showed generally faster responses (irrespective of reward or congruency) compared to SRA blocks. The behavioral benefit in these cued blocks may reflect a more pronounced global proactive cognitive control mode driven by a basic alerting function preceding target presentation ([Carrasco, 2011](#); [Coull and Nobre, 1998](#); [Posner, 1980](#)). In addition, we found a strong interference effect commonly observed in the

Stroop task across all blocks (e.g., Braver, 2012; Gonthier et al., 2016; Krebs et al., 2013). With regard to reward effects on this interference effect, results were not completely decisive. Specifically, when comparing the reward-related trials from the experimental blocks with the neutral blocks, a general reduction in interference was observed for the former. At the same time, in their direct comparison, no such differences within the reward-related blocks were clearly observed. The present data therefore seem to fall in between earlier observations of reduced interference in a reward context, e.g., in a rewarded SRA Stroop task (e.g., Krebs et al., 2013, 2010) along with conflict tasks with cued reward (e.g., Kostandyan et al., 2019; Padmala and Pessoa, 2011) and studies that have not clearly observed such effects (e.g., van den Berg et al., 2014). Such differences could relate to statistical sensitivity, but also to a whole host of experiment choices, which reward experiments feature many of. Experiment choices such as reward magnitude and probability, the frequency of feedback, the exact nature of the primary task, the implementation of performance contingency etc. (for a review see Krebs and Woldorff, 2017). While the present work represents an attempt of systematically comparing one such factor (how reward is associated to a task), many of these factors have never been formally compared.

5. Conclusions

By using cues or targets to inform participants about reward prospect in different block types, the current experiment investigated temporal and spatial aspects of the interplay between reward and cognitive control. Behaviorally, we observed stronger reward effects for SRA and C-SRA, where reward availability is linked to task-relevant factors, compared to MID. The EEG and fMRI data displayed the expected main effects of reward and congruency, generally attesting to the quality of the data (which is notable not least because our EEG cap layout did not feature a dedicated ECG channel on the participants' back), but only a limited number of findings dissociating the different block types. In particular, there was strong similarity concerning reward effects for the MID cues and the targets in the SRA and C-SRA blocks, whereas MID targets did not display strong effects in typical reward-sensitive areas. This implies similarities in how the brain responds to reward information, no matter whether it is presented in a slow pre-cued or a more immediate target-locked fashion. In addition, the C-SRA blocks identified a certain level of enhanced proactive control for the respective targets, above of what was observed for MID reward-unrelated cues, suggesting that reward effects in SRA contexts are also not brought about in a purely reactive fashion. Consistent with this, we did not observe clear differences in target processing across the different task blocks, suggesting that reward effects on cognitive-control performance might ultimately be brought about rather similarly during target processing.

Still, the fact that we did not observe a more nuanced result pattern concerning differences across the different block types might not necessarily imply full procedural unity. As noted above, the statistical power might have been relatively low, in particular for the EEG data, which tend to suffer from the MR environment. Also, being the first to tackle the comparison between these different ways of associating reward to a task, the design might have been overly complex, leading to a large number of comparisons. At the same time, other analytical approaches, e.g., a multivariate decoding or encoding approaches could have identified more fine-grained differences across the different block types, which however the current experimental design was not optimized for.

Declaration of competing interest

The authors declare no conflicts of interest.

CRediT authorship contribution statement

Mariam Kostandyan: Formal analysis, Supervision, Writing - original draft, Data curation. **Haeme R.P. Park:** Data curation. **Carsten Bundt:** Data curation. **Carlos González-García:** Formal analysis. **David**

Wisniewski: Formal analysis. **Ruth M. Krebs:** Formal analysis. **C. Nico Boehler:** Writing - original draft.

Acknowledgements

The authors would like to thank Ruth Seurinck for advice on the analysis, and Pieter Vandemaele for support during scanning. The authors also wish to acknowledge the following funding sources: the Flemish Research Foundation (FWO; grant no. 3G034315 awarded to CNB) and the European Union's Horizon 2020 Research and Innovation Program under the Marie Skłodowska-Curie (grant no. 665501 awarded to DW), as well as by a starting grant of the European Research Council (ERC) under the Horizon 2020 framework (grant No. 636116 awarded to RMK).

Appendix A. Supplementary data

Supplementary data to this article can be found online at <https://doi.org/10.1016/j.neuroimage.2020.116829>.

References

- Adcock, R.A., Thangavel, A., Whitfield-gabrieli, S., Knutson, B., Gabrieli, J.D.E., 2006. Reward-motivated learning: mesolimbic activation precedes memory formation. *Neuron* 50 (3), 507–517. <https://doi.org/10.1016/j.neuron.2006.03.036>.
- Allen, P.J., Josephs, O., Turner, R., 2000. A method for removing imaging artifact from continuous EEG recorded during functional MRI. *Neuroimage* 12 (2), 230–239. <https://doi.org/10.1006/nimg.2000.0599>.
- Anderson, B.A., Laurent, P.A., Yantis, S., 2011. Value-driven attentional capture 108 (25). <https://doi.org/10.1073/pnas.1104047108>.
- Baines, S., Ruz, M., Rao, A., Denison, R., Nobre, A.C., 2011. Modulation of neural activity by motivational and spatial biases. *Neuropsychologia* 49 (9), 2489–2497. <https://doi.org/10.1016/j.neuropsychologia.2011.04.029>.
- Banich, M.T., Milham, M.P., Atchley, R., Cohen, N.J., Webb, A., Wszalek, T., et al., 2000. fMRI studies of Stroop tasks reveal unique roles of anterior and posterior brain systems in attentional selection. *J. Cognit. Neurosci.* 12 (6), 988–1000.
- Beck, S.M., Locke, H.S., Savine, A.C., Jimura, K., Braver, T.S., 2010. Primary and secondary rewards differentially modulate neural activity dynamics during working memory. *PLoS ONE* 5 (2). <https://doi.org/10.1371/journal.pone.0009251>.
- Boehler, C.N., Schevernels, H., Hopf, J.-M., Stoppel, C.M., Krebs, R.M., 2014. Reward prospect rapidly speeds up response inhibition via reactive control. *Cognit. Affect Behav. Neurosci.* 14 (2), 593–609. <https://doi.org/10.3758/s13415-014-0251-5>.
- Botvinick, M.M., Braver, T.S., Barch, D.M., Carter, C.S., Cohen, J.D., 2001. Conflict monitoring and cognitive control. *Psychol. Rev.* 108 (3), 624–652.
- Botvinick, M.M., Braver, T.S., 2015. Motivation and cognitive control: from behavior to neural mechanism. *Annu. Rev. Psychol.* 66, 83–113. <https://doi.org/10.1146/annurev-psych-010814-015044>.
- Braver, T.S., 2012. The variable nature of cognitive control: a dual mechanisms framework. *Trends Cognit. Sci.* 16 (2), 106–113. <https://doi.org/10.1016/j.tics.2011.12.010>.
- Braver, T.S., Paxton, J.L., Locke, H.S., Barch, D.M., 2009. Flexible neural mechanisms of cognitive control within human prefrontal cortex. *Proc. Natl. Acad. Sci. U. S. A.* 106 (18), 7351–7356. <https://doi.org/10.1073/pnas.0808187106>.
- Bunzeck, N., Duzel, E., 2006. Absolute coding of stimulus novelty in the human substantia nigra/VTA. *Neuron* 51 (3), 369–379. <https://doi.org/10.1016/j.neuron.2006.06.021>.
- Burton, A.C., Nakamura, K., Roesch, M.R., 2015. From ventral-medial to dorsal-lateral striatum: neural correlates of reward-guided decision-making. *Neurobiol. Learn. Mem.* 117, 51–59. <https://doi.org/10.1016/j.nlm.2014.05.003>.
- Carrasco, M., 2011. Visual attention: the past 25 years. *Vis. Res.* 51 (13), 1484–1525. <https://doi.org/10.1016/j.visres.2011.04.012>.
- Castelhan, J., Duarte, I.C., Wibral, M., Rodriguez, E., Castelo-Branco, M., 2014. The dual facet of gamma oscillations: separate visual and decision making circuits as revealed by simultaneous EEG/fMRI. *Hum. Brain Mapp.* 35 (10), 5219–5235. <https://doi.org/10.1002/hbm.22545>.
- Chaillou, A., Giersch, A., Hoonakker, M., Capa, R.L., Bonnefond, A., 2017. Differentiating motivational from affective influence of performance-contingent reward on cognitive control: the wanting component enhances both proactive and reactive control. *Biol. Psychol.* 125, 146–153. <https://doi.org/10.1016/j.biopsycho.2017.03.009>.
- Chelazzi, L., Perlati, A., Santandrea, E., Libera, C. Della, 2013. Rewards teach visual selective attention. *Vis. Res.* 85, 58–72. <https://doi.org/10.1016/j.visres.2012.12.005>.
- Cheng, W., Rolls, E.T., Qiu, J., Liu, W., Tang, Y., Huang, C.-C., et al., 2016. Medial reward and lateral non-reward orbitofrontal cortex circuits change in opposite directions in depression. *Brain: J. Neurol.* 139, 3296–3309. <https://doi.org/10.1093/brain/aww255>.
- Chiew, K.S., Braver, T.S., 2013. Temporal dynamics of motivation-cognitive control interactions revealed by high-resolution pupillometry. *Front. Psychol.* 4, 15. <https://doi.org/10.3389/fpsyg.2013.00015>.

- Power, J.D., Petersen, S.E., 2013. Control-related systems in the human brain. *Curr. Opin. Neurobiol.* 23 (2), 223–228. <https://doi.org/10.1016/j.conb.2012.12.009>.
- Roesch, M.R., Singh, T., Brown, P.L., Mullins, S.E., Schoenbaum, G., 2009. Ventral striatal neurons encode the value of the chosen action in rats deciding between differently delayed or sized rewards. *J. Neurosci.* 29 (42), 13365–13376. <https://doi.org/10.1523/JNEUROSCI.2572-09.2009>.
- Rorden, C., Brett, M., 2000. Stereotaxic display of brain lesions. *Behav. Neurol.* 12 (4), 191–200.
- Schevernels, H., Bombeke, K., Van der Borgh, L., Hopf, J.-M., Krebs, R.M., Boehler, C.N., 2015. Electrophysiological evidence for the involvement of proactive and reactive control in a rewarded stop-signal task. *Neuroimage* 121, 115–125. <https://doi.org/10.1016/j.neuroimage.2015.07.023>.
- Schevernels, H., Krebs, R.M., Santens, P., Woldorff, M.G., Boehler, C.N., 2014. Task preparation processes related to reward prediction precede those related to task-difficulty expectation. *Neuroimage* 84, 639–647. <https://doi.org/10.1016/j.neuroimage.2013.09.039>.
- Soltani, M., Knight, R.T., 2000. Neural origins of the P300. *Crit. Rev. Neurobiol.* 14 (3–4), 199–224.
- Tachibana, Y., Hikosaka, O., 2012. The primate ventral pallidum encodes expected reward value and regulates motor action. *Neuron* 76 (4), 826–837. <https://doi.org/10.1016/j.neuron.2012.09.030>.
- Tan, J., Zhao, Y., Wu, S., Wang, L., Hitchman, G., Tian, X., et al., 2014. The temporal dynamics of visual working memory guidance of selective attention. *Front. Behav. Neurosci.* 8, 345. <https://doi.org/10.3389/fnbeh.2014.00345>.
- Tecce, J.J., 1972. Contingent negative variation (CNV) and psychological processes in man. *Psychol. Bull.* 77 (2), 73–108.
- Utevsky, A.V., Smith, D.V., Huettel, S.A., 2014. Precuneus is a functional core of the default-mode network. *J. Neurosci.: Off. J. Soc. Neurosci.* 34 (3), 932–940. <https://doi.org/10.1523/JNEUROSCI.4227-13.2014>.
- van den Berg, B., Krebs, R.M., Lorist, M.M., Woldorff, M.G., 2014. Utilization of reward-prospect enhances preparatory attention and reduces stimulus conflict. *Cognit. Affect Behav. Neurosci.* 14 (2), 561–577. <https://doi.org/10.3758/s13415-014-0281-z>.
- Visscher, K.M., Miezin, F.M., Kelly, J.E., Buckner, R.L., Donaldson, D.I., McAvoy, M.P., et al., 2003. Mixed blocked/event-related designs separate transient and sustained activity in fMRI. *Neuroimage* 19 (4), 1694–1708. [https://doi.org/10.1016/S1053-8119\(03\)00178-2](https://doi.org/10.1016/S1053-8119(03)00178-2).
- von Cramon, D.Y., Brass, M., 2002. The role of the frontal cortex in task preparation. *Cerebr. Cortex* 12 (9), 908–914. <https://doi.org/10.1093/cercor/12.9.908>.
- Wang, L., Chang, W., Krebs, R.M., Boehler, C.N., Theeuwes, J., Zhou, X., 2018. Neural dynamics of reward-induced response activation and inhibition. *Cerebr. Cortex*. <https://doi.org/10.1093/cercor/bhy275>. New York, N.Y. : 1991.
- Westbrook, A., Braver, T.S., 2015. Cognitive effort: a neuroeconomic approach. *Cognit. Affect Behav. Neurosci.* 15 (2), 395–415. <https://doi.org/10.3758/s13415-015-0334-y>.
- Wisniewski, X.D., Reverberi, C., Momennejad, I., Kahnt, X., Haynes, J., 2015. The role of the parietal cortex in the representation of task – reward associations, 35, pp. 12355–12365. <https://doi.org/10.1523/JNEUROSCI.4882-14.2015>, 36.
- Yee, D.M., Braver, T.S., 2018. Interactions of motivation and cognitive control. *Curr. Opin. Behav. Sci.* 19, 83–90. <https://doi.org/10.1016/j.cobeha.2017.11.009>.
- Zhang, S., Li, C.-S.R., 2014. Functional clustering of the human inferior parietal lobule by whole-brain connectivity mapping of resting-state functional magnetic resonance imaging signals. *Brain Connect.* 4 (1), 53–69. <https://doi.org/10.1089/brain.2013.0191>.